Electronic Supplementary Information (ESI)

Gold Nanoshell Coated Thermo-pH Dual Responsive Liposomes for Resveratrol Delivery and Chemo-photothermal Synergistic Cancer Therapy

*Meili Wang[a], Yanping Liu[a], Xuwu Zhang[a], Liyao Luo[a], Lei Li[a], Shanshan Xing[a,b], Yuchu He[a], Weiwei Cao[a], Ruiyan Zhu[a], Dawei Gao[a,b]**

[a] Applying Chemistry Key Lab of Hebei Province, Yanshan University, No.438 Hebei Street, Qinhuangdao, 066004, China.

[b] Hebei Province Asparagus Industry Technology Research Institute, Qinhuangdao, 066318, China.

Correspondence:

TEL: +86 335 8387553; FAX: +86 335 8387553;

Email: dwgao@ysu.edu.cn

1. Materials

1.1. Materials and instruments

$AuCl_3$ was obtained from the Chengdu Xiya Chemical Industry Co., Ltd (Chengdu, China). $NaBH_4$ was purchased from Tianjin Guangfu Fine Chemicals Co., Ltd (Tianjin, China). Resveratrol was acquired from J Co (Jiangsu, China). Soya phosphatidyl choline (SPC) and cholesterol were supplied by henyang Tianfeng Biological Pharmaceutical Co., Ltd. (Shenyang, China) and Tianjin Guangfu Fine Chemical Research Institute (Tianjin, China) respectively. Chitosan (degree of deacetylation: 92%) was purchased from Sinopharm Chemical Reagent Co., Ltd (Shanghai, China). Unless otherwise stated, all the chemicals and reagents were of analytical grade and used without further purification. Deionized water with a resistivity of 18.2 MΩ·cm was from Milli-Q Water Purification System.

1.2. Preparation of Res-liposomes

Liposomes were prepared based on the ethanol injection method. Briefly, the mixture of SPC:Chol:Res (50:6:5 molar ratio) was completely dissolved in ethanol absolute as the lipid phase, Tween-80 (0.1%, v/v) was dissolved in 10 mL phosphate-buffered saline (PBS, pH 6.5, 0.01 M) at 43 °C as the aqueous phase. Then, the lipid phase was dropped into the aqueous phase under mild magnetic stirring. The residual ethanol was evaporated by a shaking table until a homogeneous dispersion was formed.

1.3 Preparation of Au NPs

Au seeds were prepared as the following method: briefly, $AuCl_3$ solution (20 mM, 1 mL) was diluted to 0.5 mM with deionization water at 4°C. Next, 10 μL of fresh 253 mM ice cold $NaBH_4$ solution was added. The solution turned orange-pink immediately, indicating particle formation. Then the Au seeds were aged for 30 min at room temperature. The Au NPs solution was sonicated (20 W, 20 kHz) for 10 s to avoid any kind of particle aggregation.

1.4 Preparation of Au growth solution

Au growth solution was prepared by dissolving 0.015 g of K_2CO_3 in 9 mL of deionized water and subsequent addition of 1 mL of 0.02 M $AuCl_3$; then the solution aged for 24 h with pH = 10. At this pH value, the coordination compound of $AuCl_3$ is stable $[Au(OH)_4]^-$, therefore, the self-nucleation would be inhibited, and the present gold nuclei could grow larger to form compact gold nanoshells[1].

1.5 Characterizations of GNS@CTS@Res-lips

The nano drug carriers were subjected to the following characterization techniques. The mean diameter, particle size distribution, and zeta potential were measured by Malvern Zetasizer Nano (Malvern; Worcestershire, U.K.). The delivery system morphology was detected by a transmission electron microscope (TEM, HT-

7700, Japan) followed by negative staining procedure using phosphotungstic acid. UV-vis spectra were measured by a UV-vis spectrophotometer (UV-2550, Shimadzu, Japan). Fourier transform infrared (FTIR) spectra over a frequency range of 4000 to 400 cm^{-1} was recorded to analyze functional groups on the samples using a Fourier transform infrared spectrometer (Nicolet iS10, USA) with the KBr method (the samples were prepared by processing compressed KBr disks at room temperature before detection and analysis). In addition, the amount of Au on the liposomal surface was determined by inductively coupling plasma mass spectrometry (ICP-MS). X-ray diffraction (XRD) patterns were recorded with a GADDS diffractometer (Rigaku-SmartLab 2500, Japan)

The encapsulation efficiency (EE) was calculated from the following formula:

$$EE\ (\%) = (W_{en} / W_{total}) \times 100\%$$

Where W_{en} was the amount of encapsulated drug, and W_{total} was the amount of total drug.

1.6 drug release from drug carriers

The release of Res from liposomes was investigated by dialysis method. Briefly, the samples of Res-lips, CTS@Res-lips and GNS@CTS@Res-lips (1 mL) were placed in a dialysis bag (MWCO 12,000 - 14,000), respectively. Then, the dialysis bags were immersed separately in 200 mL PBS buffer at pH 5.0 or 7.4 containing 0.1% (v/v) Tween 80 and incubated with continuous stirring at 37 °C water bath. The samples (1 mL) were taken from the dialysis bags at the predetermined time intervals (1, 2, 4, 8, 12, 16, 20 and 24 h), and the drug content of each sample was analyzed by high performance liquid chromatography (HPLC).

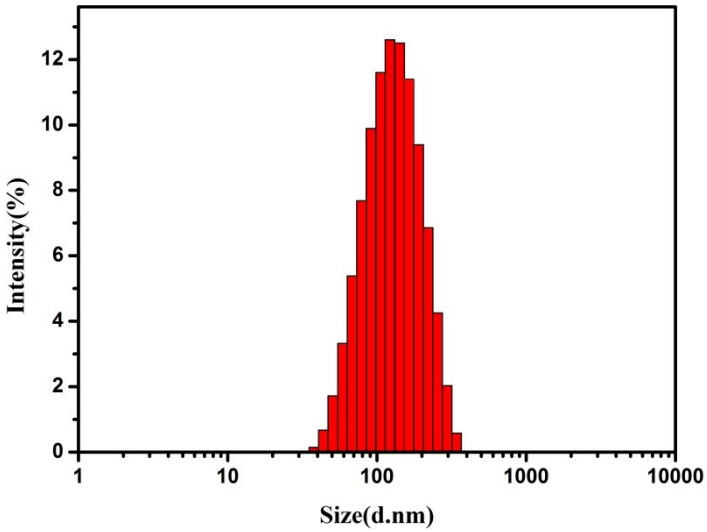

Figure S1. Particle size distribution of Res-lips by DLS.

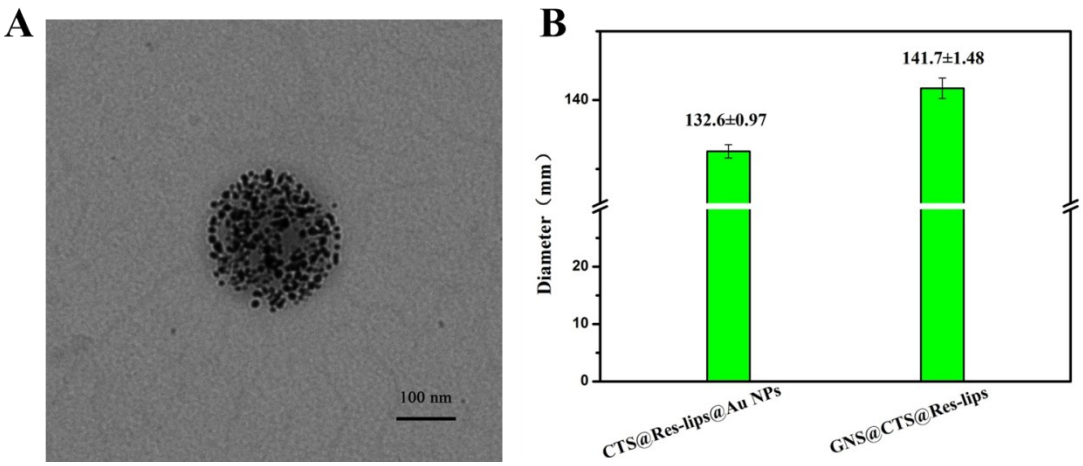

Figure S2. (A) TEM image of Au seeds coated CTS@Res-lips (CTS@Res-lips@Au NPs). (B) DLS size analysis of CTS@Res-lips@Au NPs and GNS@CTS@Res-lips

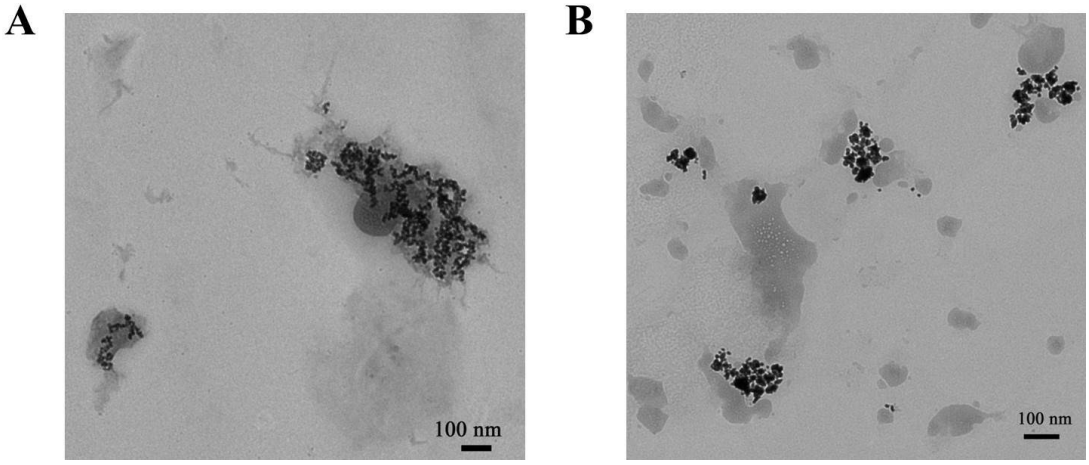

Figure S3. Storage stability GNS@CTS@Res-lips: TEM image of GNS@CTS@Res-lips after storage at 25°C (A) and 37°C (B) for one month.

2 Results and discussion

2.1 Photothermal conversion efficiency

To further precisely demonstrated the photothermal conversion capabilities of the synthesized GNS@CTS@Res-lips, the photothermal conversion efficiency (η), which was an important parameter for characterizing the PTT agents and played a key role in the PTT, was estimated. The temperature change of the GNS@CTS@Res-lips was recorded under continuous irradiation of the 808 nm laser with a power density of 2 W for 10 min. A change in the course of the temperature plot with time was recorded and depicted in Figure S4, which showed that the temperature increased from 25.0 °C to a maximum temperature of 66.7 °C within 10 min of irradiation, and then gradually decreased to ambient temperature after turning off the laser. The photothermal conversion efficiency (η), was calculated according to the previous reported method[2-4]

$$\eta = \frac{hS(T_{max} - T_{surr}) - Q_{dis}}{I(1 - 10^{-A_{808}})} \quad (1)$$

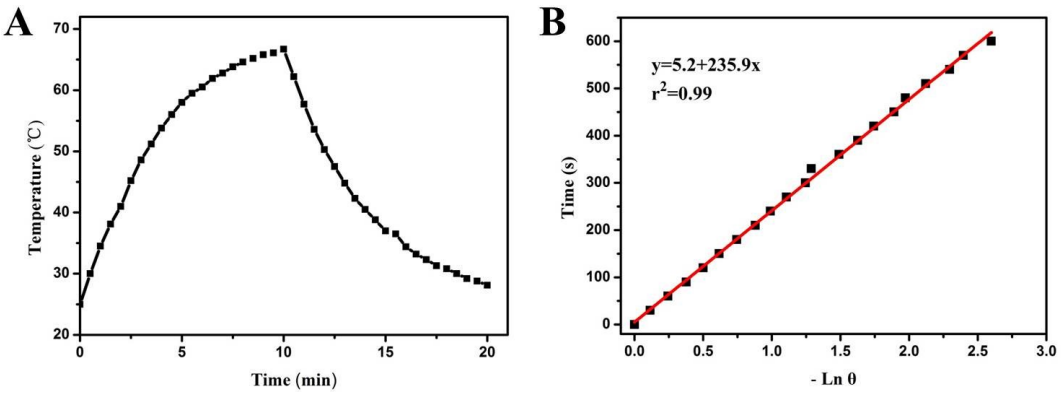

Figure. S4 (A) Temperature evolution plot of GNS@CTS@Res-lips upon irradiation for 10 min (808 nm, 2.0 W) and then shutting off the laser. (B) Plot of cooling time as a function of negative natural logarithm of the temperature driving force obtained from the cooling stage.

In this equation, h is heat transfer coefficient, S is the contacting area between container and environment, Q_{diS} express the heat associated with the light absorbance, which can calculate by $Q_{dis}=hS\,(T_{max,water} - T_{surr,water})$. I express the incident laser power, A_{808} is the absorbance of the GNS@CTS@Res-lips at 808 nm, T_{max} is the highest temperature that can be reached under irradiation, and T_{surr} is the surrounding temperature. The value of hS can be derived from the following equation (2) to (3)

$$\tau_S = \frac{m_D C_D}{hS} \tag{2}$$

Where τ_s mean the sample system time constant, m_D and C_D express the mass (0.5 g) and heat capacity 4.2 J/(g·°C), when deionized water is used as the solvent. The time constant, τ_s, was defined as the slope of cooling time against -ln(θ) (Figure S4B), where θ is the temperature driving force, which is defined by eq 3:

$$\theta = \frac{T_{surr} - T}{T_{surr} - T_{max}} \tag{3}$$

Therefore, time constant for heat transfer from the system was determined to be τ_s =235.9 s by applying the linear time data from the cooling period (after 10 min) *vs* -lnθ (Figure S4B). In addition, the value of m and C_p were 0.5 g and 4.2 J/(g·°C). Thus, according to Equation (2), the hS was calculated to be 8.9 mW/°C. Substituting all of value to parameters into the equation (1), the photothermal conversion efficiency of GNS@CTS@Res-lips can be calculated to be 31.8%, which was higher than that of gold nanorods (21%)[5], Cu-based complex nanoparticles (16.3%)[6] and other polymer photothermal agents.

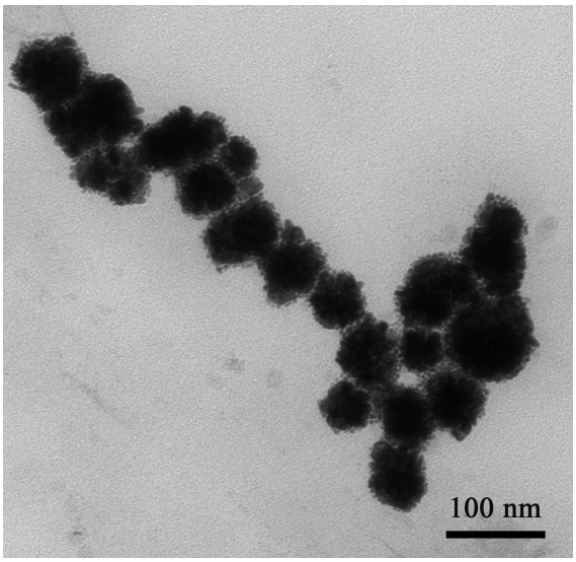

Figure S5. TEM image of GNS@CTS@Res-lips after 5 on/off cycles of 808 nm laser irradiation.

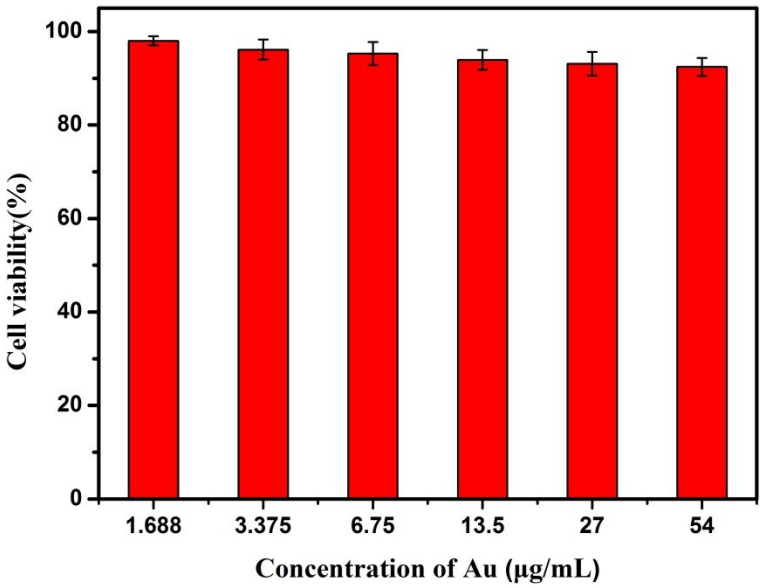

Figure S6. Cell viability of HeLa cells incubated with different concentrations of GNS@CTS@lips nanoplates for 24 h.

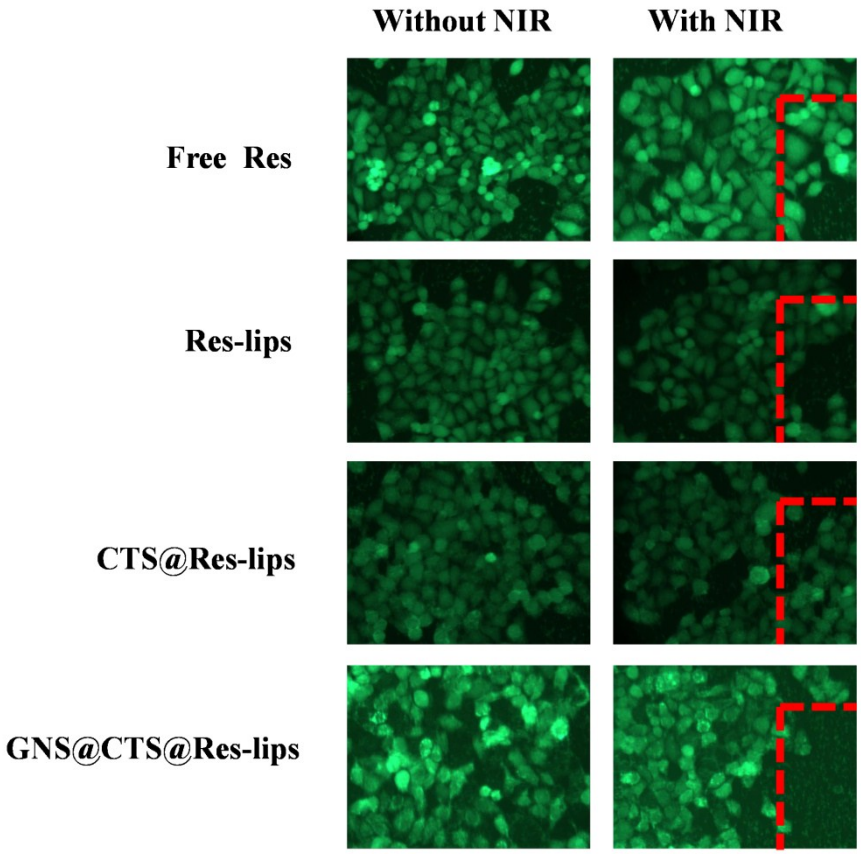

Figure S7. Fluorescence microscopy images of HeLa cells with different treatments via staining with FDA.

Notes and references

1 X. Wang, H. Liu, D. Chen, X. Meng, T. Liu, C. Fu, N. Hao, Y. Zhang, X. Wu, J. Ren and F. Tang, *ACS Appl. Mater. Inter.,* 2013, **5**, 4966-4971.

2 P. Huang, J. Lin, W. Li, P. Rong, Z. Wang, S. Wang and R. D. Leapman, *Angew. Chem.,* 2013, **125**, 14208-14214.

3 L. Zhang, Y. Chen, Z. Li, L. Li, P. Saint-Cricq, C. Li, J. Lin, C. Wang, Z. Su and J. I. Zink, *Angew. Chem.,* 2016, **55**, 2118-2121.

4 M. Ji, M. Xu, W. Zhang, Z. Yang, L. Huang, J. Liu, Y. Zhang, L. Gu, Y. Yu, W. Hao, P. An, L. Zheng, H. Zhu and J. Zhang, *Adv. Mater.,* 2016, **28**, 3094-3101.

5 C. M. Hessel, V. P. Pattani, M. Rasch, M. G. Panthani, B. Koo, J. W. Tunnell and B. A. Korgel, *Nano Lett.*, 2011, **11**, 2560-2566.

6 S. Wang, A. Riedinger, H. Li, C. Fu, H. Liu, L. Li, T. Liu, L. Tan, M. J. Barthel and G. Pugliese, *ACS Nano*, 2015, **9**, 1788-1800.